ARTICLE

OBC
www.rsc.org/obc

New pyrimidine- and fluorene-containing oligo(arylene)s: synthesis, crystal structures, optoelectronic properties and a theoretical study †

Gregory Hughes,[a] Changsheng Wang,[a] Andrei S. Batsanov,[a] Michael Fern,[a] Stephen Frank,[a] Martin R. Bryce,*[a] Igor F. Perepichka,[b] Andrew P. Monkman[c] and Benjamin P. Lyons[c]

[a] *Department of Chemistry, University of Durham, South Road, Durham, UK DH1 3LE. E-mail: m.r.bryce@durham.ac.uk; Fax: 44 191 384 4737*

[b] *L. M. Litvinenko Institute of Physical Organic and Coal Chemistry, National Academy of Sciences of Ukraine, Donetsk 83114, Ukraine*

[c] *Department of Physics, University of Durham, South Road, Durham, UK DH1 3LE*

Received 23rd May 2003, Accepted 30th June 2003
First published as an Advance Article on the web 28th July 2003

New pyrimidine containing oligo(arylene)s, notably the pyrimidine–fluorene hybrid systems **13**–**16**, have been synthesised by Suzuki cross-coupling methodology. An efficient synthesis of the key reagent 9,9-dihexylfluorene-2,7-diboronic acid **10** from 2,7-dibromo-9,9-dihexylfluorene **9** is reported. Cross-coupling of **10** with two equivalents of 2-bromopyrimidine, 5-bromopyrimidine and 2,5-dibromopyrimidine gave 2,7-bis(2-pyrimidyl)-9,9-dihexylfluorene **13**, 2,7-bis(5-pyrimidyl)-9,9-dihexylfluorene **14** and 2,7-bis(5-bromo-2-pyrimidyl)-9,9-dihexylfluorene **15** in 23–34% yields. A further two-fold Suzuki reaction of benzeneboronic acid with compound **15** gave 2,7-bis(5-phenyl-2-pyrimidyl)-9,9-dihexylfluorene **16** (35% yield). *Ab initio* calculations of the geometries and electronic structures at the Hartree–Fock (HF) and density functional theory (DFT) levels of theory are reported for compounds **13**, **14** and **16** (with ethyl substituents replacing hexyl) and for their dipyrazinyl and bistetraazenyl analogues, **17**, **18**, **20** and **21**. The heterocyclic nitrogen atoms of **13** and **16** facilitate planarisation of the system, compared to **14**, which is in agreement with X-ray structural data obtained for 5-bromo-2-phenylpyrimidine **6**, 2,5-diphenylpyrimidine **7** and compound **15**. Bistetrazenyl derivative **21** is calculated to be a fully planar system. The cyclic voltammogram (CV) of compound **16** in dichloromethane solution shows a quasi-reversible oxidation wave at $E_{1/2}^{0} = +1.36$ V (*vs.* Ag/Ag^{+}). Compound **13** is a poorer donor with an oxidation observed at $E_{pa} = +1.50$ V which is in good agreement with the difference in the energies of their HOMO orbitals calculated at both HF and DFT levels of theory (0.11–0.12 eV). For compound **14** we were not able to measure an E_{ox} potential which should lie at much more positive potentials. Compounds **15** and **16** are blue emitters in solution, with photoluminescence quantum yields (PLQY) of 25% and 85%, respectively. For thin films of **16** the PLQY is reduced to 21%. An OLED using compound **16** as the emissive layer has been fabricated in the configuration ITO/PEDOT/**16**/Ca/Al: blue-green light (λ_{max} 500 nm) most likely emanating primarily from excimer states is emitted at a high turn-on voltage.

Introduction

Studies on the synthesis, structural ordering and optoelectronic properties of conjugated oligo- and poly(aryl/heteroaryl) systems are central to the development of new materials for electronics and photonics applications,[1] *e.g.* as components of organic light emitting devices (OLEDs) for displays and lighting,[2] and field effect transistors (FETs).[3] In the search for materials with improved electron transport properties, the insertion of electron-deficient heterocycles,[4] *e.g.* 1,3,4-oxadiazole,[5] pyridine,[6] quinoline,[7] quinoxaline and pyridopyrazine[8] into conjugated oligomer/polymer backbones has been implemented. This approach has been used to tune luminescence properties in solution and in the solid state and to balance charge injection from electrodes in OLED structures.

It is surprising that pyrimidine units have been only very rarely incorporated into conjugated oligomer or polymer structures.[5c,9,10] For example, poly(2,5-pyrimidinylene) **1** is an electron accepting material which can be doped with sodium to obtain an n-type semiconductor;[9a] a 1,3,4-oxadiazole–pyrimidine hybrid oligo(arylene) **2** has been shown to function as an electron conducting/hole blocking (ECHB) layer in bilayer LEDs using poly[2-methoxy-5-(2-ethylhexyloxy)-1,4-phenylene-vinylene] (MEH-PPV) as the emissive material,[5c] and during the preparation of this manuscript it was reported that the spirobifluorene–pyrimidine hybrid **3** (Chart 1) is a blue emitter.[9b]

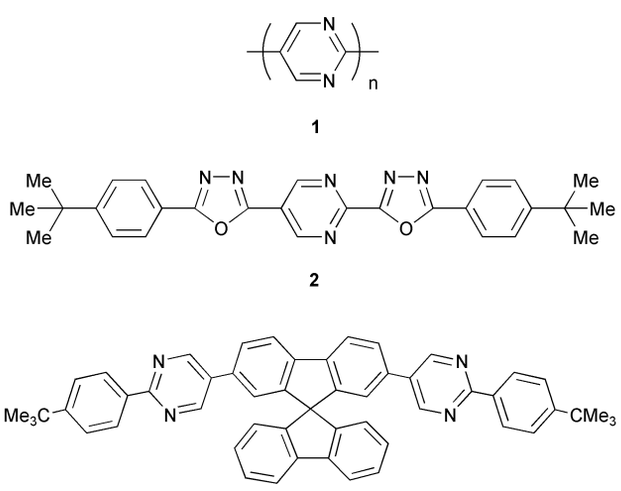

1 **2** **3**

Chart 1

Pyrimidine was attractive to us for two main reasons: (i) it has a higher electron affinity than pyridine;[10] and (ii) due to the lack of *ortho–ortho* interactions of C–H hydrogens, 2-aryl-

† Electronic supplementary information (ESI) available: experimental synthetic procedures for compounds **4**, **9** and **10**; HF/6–31G(d,p) and B3LYP/6–31G(d,p) calculated geometries and frontier orbitals for compounds **13E**, **14E** and **16E**–**21E**. See http://www.rsc.org/suppdata/ob/b3/b305870k/

DOI: 10.1039/b305870k

pyrimidine derivatives should be more planar (*i.e.* possess increased π–conjugation) compared with 2-arylpyridine (or biphenyl) analogues. Our initial aim, therefore, was to develop efficient syntheses of new and versatile functionalised pyrimidines, especially pyrimidine-containing oligo(arylene) systems, and herein we report the synthesis of such compounds, namely **7** and **13**–**16**. We also describe the X-ray crystal structures of **6**, **7** and **15**, *ab initio* calculations, optical absorption and photoluminescence spectra, and OLED studies using compound **16** as the emissive layer. The fluorenyl core of **13**–**16** was chosen because of its known high stability and luminescence efficiency, with the alkyl chains at C(9) imparting good solubility in organic solvents.[11,12]

Results and discussion

Synthesis

Suzuki cross-coupling methodology is a very versatile route to oligo(arylene)s[13] and for this we required 2,5-dibromopyrimidine **4** as a starting material. We readily obtained **4** in 29% yield from commercial 2-hydroxypyrimidine hydrochloride and found our procedure (see electronic supplementary information (ESI) †) to be considerably more convenient than the literature routes.[14] There are very few examples of Suzuki reactions on halopyrimidines,[15] so as a test reaction, we treated **4** with benzeneboronic acid **5** (3.0 equivalents) in the presence of catalytic $Pd(PPh_3)_4$ in refluxing tetrahydrofuran (THF) (Scheme 1) and obtained two products which were easily separated and identified as 2-phenyl-5-bromopyrimidine **6** (43% yield) and 2,5-diphenylpyrimidine **7** (32% yield), both of which had been obtained previously by different routes.[16] This reaction is of fundamental interest in that it established that the bromine atom at C(2) of compound **4** is more labile under standard Suzuki conditions. Compound **7** was obtained in higher yield (62%) using benzeneboronic acid **5** (2.0 equivalents) and $Pd_2(dba)_3$ catalyst[17] at 20 °C.

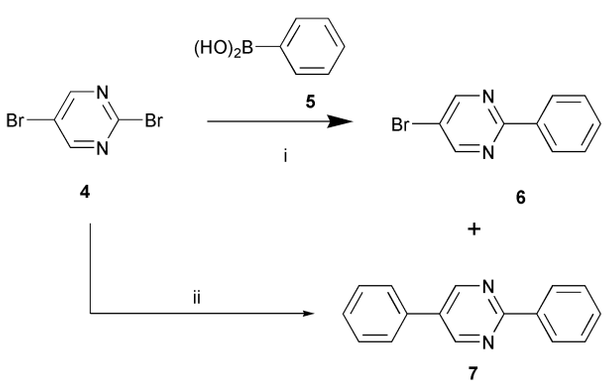

Scheme 1 *Reagents and conditions*: (i) compound **5**, $Pd(PPh_3)_4$, THF, Na_2CO_3, reflux; (ii) compound **5**, $Pd_2(dba)_3$, $P(Bu^t)_3$, THF, 20 °C.

2,7-Dibromo-9,9-dihexylfluorene **9** was obtained in 85% yield from commercial dibromofluorene **8** by deprotonation with potassium *t*-butoxide followed by alkylation with bromohexane (Scheme 2).[18] This procedure seems more convenient than the two-step route from fluorene (alkylation, then bromination) reported by several groups.[11b,12] 9,9-Dihexylfluorene-2,7-diboronic acid **10**, which is a key reagent for many fluorene-based luminophores, was obtained in 86% yield from **9** by reaction with *n*-butyllithium and triisopropylborate, followed by aqueous workup.[19] All the data obtained for **9** and **10** confirm no detectable contamination with unwanted fluorenone byproducts. Compound **10** is a shelf-stable solid, and its reaction with two equivalents of 2-bromopyrimidine **11**, 5-bromopyrimidine **12** and 2,5-dibromopyrimidine **4**, as above, gave **13**, **14** and **15** in 34, 32 and 23% yields, respectively. A further two-fold Suzuki reaction of benzeneboronic acid with compound **15** afforded the hexa(arylene) system **16** (35% yield) bearing terminal phenyl groups. The low yield of pure product from this capping reaction was primarily due to difficulties in the purification of **16**.

Crystal structures of compounds 6, 7 and 15‡

Molecule **6** is twisted around the C(2)–C(11) bond by 18.3° (Fig. 1) which is smaller than that observed in biphenyl (see discussion below), thus confirming that nitrogen atoms facilitate planarisation of the system. Molecule **7** is located on a crystallographic twofold axis, normal to the long axis of the molecule. The central pyrimidine ring is disordered between two orientations, related *via* this axis and forming an interplanar angle of 14.8°. In each case, the pyrimidine ring is inclined by 19.8° and 34.6° to the phenyl groups in positions 2 and 5, respectively (Fig. 2) which reflects the same tendency of planarisation of the system *via* substitution of C–H by nitrogen atoms in oligophenylenes. In molecule **15** the fluorene moiety is planar, while the pyrimidine rings bonded to C(4) and C(10) are inclined to its plane by 5.1° and 5.6°, respectively (Fig. 3). These angles are much smaller that those observed for **6** and **7**, which could be a result of better conjugation of the pyrimidine rings with the central planar fluorene core in this extended π-system. One *n*-hexyl chain entirely and the other one nearly [with the exception of the terminal C(33) atom], adopt an all-*trans* conformation and lie in one plane, perpendicular to the fluorene plane.

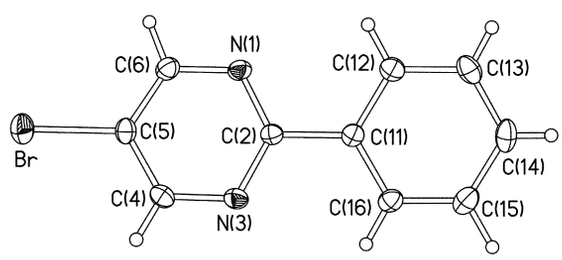

Fig. 1 Molecular structure of **6** (henceforth thermal ellipsoids are drawn at 50% probability level).

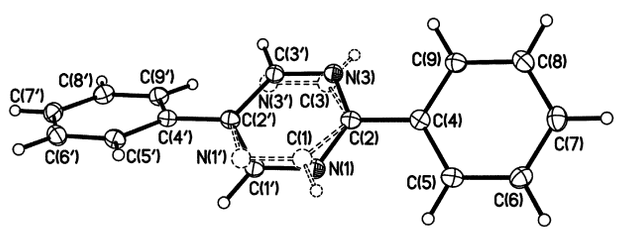

Fig. 2 Molecular structure of **7**, showing the disorder of the pyrimidine ring. Atoms, symmetrically dependent *via* the twofold axis, are primed.

In an isolated molecule, the twist angle (ω) between two bonded aromatic rings depends on the balance between π conjugation (which favours planarity) and steric repulsion between H atoms (or substituents) in *peri*-positions. For the latter, heteroatoms and substituents in *meta*- and *para*-positions are largely irrelevant. Hence a 5-phenylpyrimidine (or 5,5-bispyrimidine) moiety (type A link) can be expected to behave in the same way as the biphenyl molecule, which has potential barriers (albeit low, 2 to 2.5 kcal mol^{-1}) at both $\omega = 0$ and $\omega = 90°$,[20] and the stable conformation with an intermediate twist, as observed in the gas phase by electron diffraction ($\omega = 45°$),[21] Raman ($\omega = 25°$)[22] or electron spectroscopy ($\omega = 40°$),[20d] as well as in solutions and melts ($\omega = 32 \pm 2°$).[23] Although in the solid

‡ CCDC reference numbers 203937–203939. See http://www.rsc.org/suppdata/ob/b3/b305870k/ for crystallographic data in .cif or other electronic format.

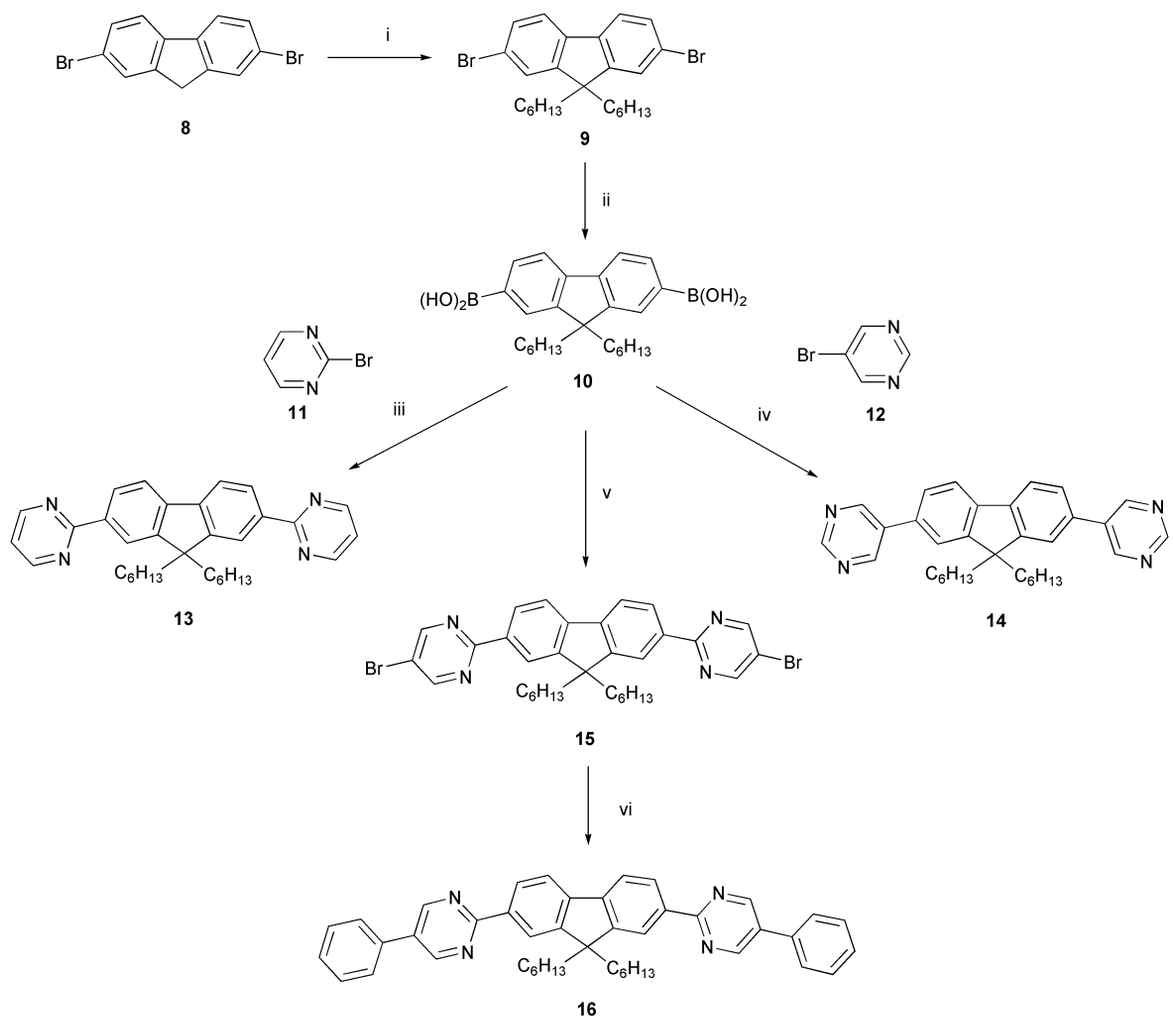

Scheme 2 *Reagents and conditions*: (i) 1-bromohexane, *t*-BuOK, THF, 0⟶ 20 °C; (ii) *n*-BuLi, THF, −78 °C, triisopropylborate; −78⟶20 °C, then H_2O; (iii) compound **11**, THF, $Pd(PPh_3)_4$, Na_2CO_3, reflux; (iv) compound **12**, THF, $Pd(PPh_3)_4$, Na_2CO_3, reflux; (v) compound **4**, THF, $Pd(PPh_3)_4$, Na_2CO_3, reflux; (vi) compound **5**, THF, $Pd(PPh_3)_4$, Na_2CO_3, reflux.

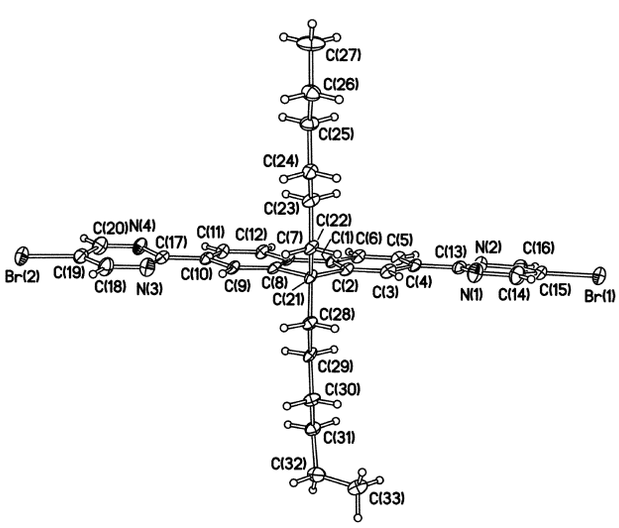

Fig. 3 Molecular structure of **15**.

state the molecule lies at a crystallographic inversion centre (which implies planarity) there are indications of disorder, so that the actual conformation is probably a slightly twisted one,[24] as in fact is observed in the non-centrosymmetric low-temperature phase.[20a] In any case, a 2-phenylpyrimidine moiety (type B link) lacks the main driving force for twisting, the pyrimidine having no peri-H atoms. Indeed, in eight previously studied structures with sterically unhindered 2-phenylpyrimidine moieties,[10,25] the dihedral angle between the phenyl and pyrimidine rings varies from 0 to 14.5°. Four of these contain simultaneously A and B type links, and present two different conformations. In 2-(4-*n*-propoxyphenyl)- and 2-(4-*n*-butoxyphenyl)-5-phenylpyrimidines[25b] and 1,4-bis(5-phenyl-2-pyrimidinyl)-phenylene[10] the B-link is twisted much more (35–39°) than the A-link (3–9°); while in 2-phenyl-5-(4-*n*-pentoxyphenyl)pyrimidine[25d] *both* A and B-twists are small (6–9°) and the molecule is approximately planar.

Optical absorption and photoluminescent properties

Solution UV-Vis absorption photoluminescence (PL) spectra for **13**–**16** were recorded in DCM. There is a progressive red shift in the value of λ_{max} of the low energy band in the sequence **14** (328 nm), **13** (352.5 nm), **15** (365 nm) and **16** (371.5 nm) (Fig. 4, Table 1). HOMO–LUMO energy gaps (E_g) estimated

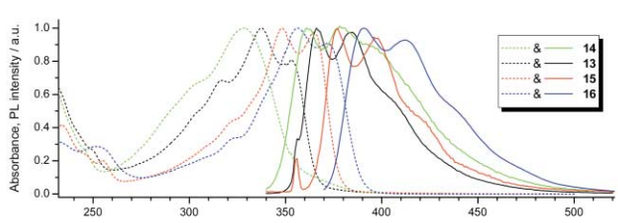

Fig. 4 Normalised UV–Vis absorption (dashed lines) and PL (solid lines) (excitation at 355 nm) spectra for compounds **13**–**16** in DCM, 20 °C.

Table 1 Absorption and emission λ_{max} values for compounds in dichloromethane, 20 °C

Compound	Absorption, λ_{max}/nm	PL, λ_{max}/nm
13	317.0, 337.5, 352.5	366, 384
14	328.0	361, 378
15	348.0, 365.0	377, 396
16	356.5, 371.5	391, 412

from the low-energy absorption edge are 3.39, 3.47, 3.28 and 3.13 eV, for compounds **14**, **13**, **15** and **16**, respectively. This order of E_g evolution is expected: twisting between pyrimidine and fluorene rings in compound **14** as compared to its planar isomer **13** (see calculation section below) hinders electron delocalisation and therefore resulst in an increase of E_g, whereas π-extension of the system by attaching additional phenyl rings to **13** to give **16** leads to E_g contraction. This trend in HOMO–LUMO gap changes is well reproduced by *ab initio* calculations (see below).

The λ_{max} values for the emission spectra obtained by excitation at 355 nm are also red shifted in the same order as the absorption spectra (Fig. 4, Table 1). The photoluminescence quantum yields (PLQY) for **15** and **16** in DCM solution were 25% and 85%, respectively. The high PLQY value obtained for **16** is consistent with that observed in other fluorene-containing oligomers,[11,26] and, importantly, confirms that the presence of the pyrimidine units is not detrimental to the high luminescence efficiency of the fluorene moiety. It has been reported that when some heterocyclic segments, *e.g.* 2,1,3-benzothiadiazoles, are incorporated into poly(fluorene) chains the fluorene photoluminescence is completely quenched due to exciton confinement.[27] The considerably lower PLQY value for **15** can be explained by quenching of the emission by the bromine substituents.

The PL spectra of solution and thin film of **16** (Fig. 5) show well-structured emission bands with λ_{max} = 414 nm (toluene solution) and 418, 440 nm (film). We calculate a solid state PLQY of 21%, similar to that of many polyfluorenes.[11]

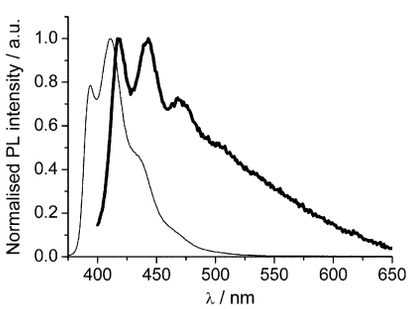

Fig. 5 Photoluminescence spectra of **16** in toluene solution (thin line) and solid state (thick line). Excitation was at 350 nm.

Light emitting device studies

The light-emitting diodes comprising a thin film (300 nm) of compound **16**, sandwiched between poly(ethylenedioxythiophene) (PEDOT)-coated ITO glass and Ca electrodes, ITO/PEDOT/**16**/Ca/Al, were fabricated. These devices had turn-on voltages of 40–50 V, such that an electric field of ~1.5 MV cm^{-1} (typical for this class of material)[28] was required to achieve electroluminescence (EL). This luminescence was blue-green (λ_{max} 500 nm) and of low intensity (Fig. 6). This low-energy emission is absent from the PL spectra of the solution, suggesting that it arises from aggregates in the film.[29] To support this point, Fig. 6 also shows the difference between the PL in solid state and in solution. This represents emission from dimeric states in the film which are not present in the solution. As the film absorption spectrum (not shown) shows no evidence of a corresponding ground state absorption to the red side of the

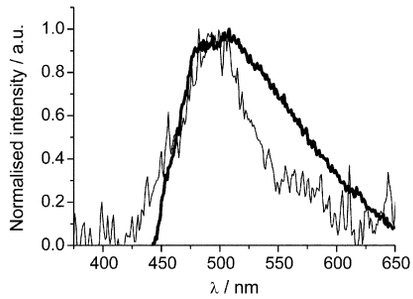

Fig. 6 Electroluminescence spectra (thin line) and excimer emission (thick line) from **16**. The excimer emission was calculated by first red-shifting the solution photoluminescence by 31 nm, such that the emission modes coincided with those in the solid state. The spectra were then normalised and the solution emission was subtracted from that of the thin film.

π–π* absorption band, these states are most likely to be excimers, which are formed by strong coupling between excited and ground state molecules, and usually have very low quantum yields. Small molecules like **16** (as opposed to polymers) are renowned for excimer formation.[30] We can discount the presence of defect sites (*e.g.* ketones which can be formed during the operation of polyflyorene-based LEDs[31]) as the source of low EL intensity as related fluorene-based compounds synthesised in our laboratory have been shown not to possess these defects.[32] There is a reasonable match between this excimer emission and the EL spectra, supporting our claim that EL emanates from these excimer states. The high turn-on voltage and low intensity of the emission will preclude practical device applications, so we have not explored **16** further in this context.

Electrochemical properties

The electrochemical behaviour of compounds **13**, **14**, and **16** was studied by cyclic voltammetry (CV) in DCM solution at room temperature using Bu_4NPF_6 (0.2 M) as supporting electrolyte. The CV of compound **16** (Fig. 7) shows a quasi-reversible (ΔE_{pa-pc} = 120 mV) oxidation peak at $E^0_{1/2}$ = +1.36 V (*vs.* Ag/Ag$^+$). Compared to compound **16**, compound **13** is a poorer donor with an oxidation observed at higher potentials. Moreover, the oxidation process becomes irreversible showing only an anodic peak at E_{pa} = +1.50 V (at 100 mV s^{-1}) [in addition, the adsorption of the material on the electrode surface occurs during the CV experiment, so the current at further scans is decreased]. The observed difference in E_{pa} values between **13** and **16** (1.50–1.42 = 0.08 V) is in good agreement with the difference in the energies of their HOMO orbitals calculated at both Hartree–Fock (HF) and density functional theory (DFT) levels of theory (0.11–0.12 eV, Table 2). For compound **14** we were not able to measure an E_{ox} potential which should lie at much more positive potentials.

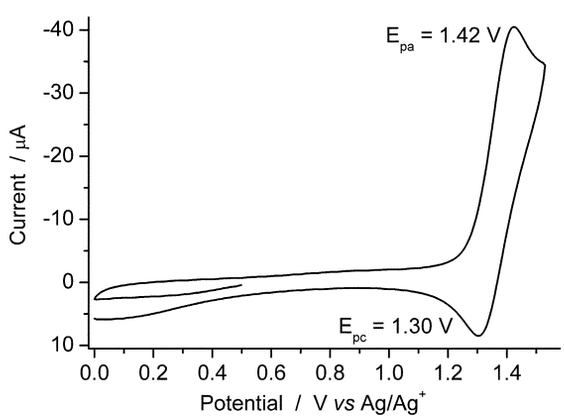

Fig. 7 Cyclic voltammogram of compound **16** in 0.2 M Bu_4NPF_6–DCM, scan rate 100 mV s^{-1}, 20 °C.

Table 2 Calculated energy parameters and dihedral angles for compounds **13E**,**14E**, and **16E**–**21E**

Compound	E_h/ hartree	LUMO/ eV	HOMO/ eV	$\Delta E_{HOMO-LUMO}$/ eV	ω_1 (°)/ω_2 (°) [a]
HF/6-31G(d,p)					
13E	−1177.40334	+1.74	−7.36	9.10	0.0
14E	−1177.38722	+1.86	−7.81	9.67	45.3
17E	−1177.37228	+1.70	−7.52	9.21	28.9
18E	−1241.19547	+1.04	−8.00	9.04	0.0
16E	−1636.52019	+1.64	−7.24	8.88	0.5/44.7
19E	−1636.51919	+1.71	−7.55	9.26	44.4/0.6
20E	−1636.49503	+1.54	−7.28	8.82	27.6/27.7
21E	−1700.32632	+0.97	−7.68	8.65	0.1/0.1
B3LYP/6-31G(d,p)					
13E	−1184.98926	−1.80	−5.60	3.80	0.0
14E	−1184.97407	−1.86	−6.01	4.15	37.5
17E	−1184.96753	−1.95	−5.77	3.82	20.1
18E	−1248.98090	−2.88	−6.30	3.42	0.0
16E	−1647.11847	−1.90	−5.48	3.58	0.2/36.7
19E	−1647.11750	−1.94	−5.74	3.80	36.2/0.2
20E	−1647.10330	−2.05	−5.55	3.50	18.5/18.9
21E	−1711.12568	−2.65	−5.97	3.32	0.0/0.0
B3PW91/6-31G(d,p)					
13E	−1184.54102	−1.90	−5.72	3.82	0.0
14E	−1184.52583	−1.96	−6.13	4.17	38.3
17E	−1184.51868	−2.05	−5.90	3.85	20.8
18E	−1248.50605	−2.96	−6.42	3.46	0.0
16E	−1646.49303	−2.01	−5.61	3.61	0.1/37.6
19E	−1646.49199	−2.05	−5.87	3.82	36.9/0.1
20E	−1646.47718	−2.16	−5.68	3.52	18.5/19.4
21E	−1710.47354	−2.74	−6.10	3.35	0.0/0.0

[a] Dihedral angles, see Chart 2.

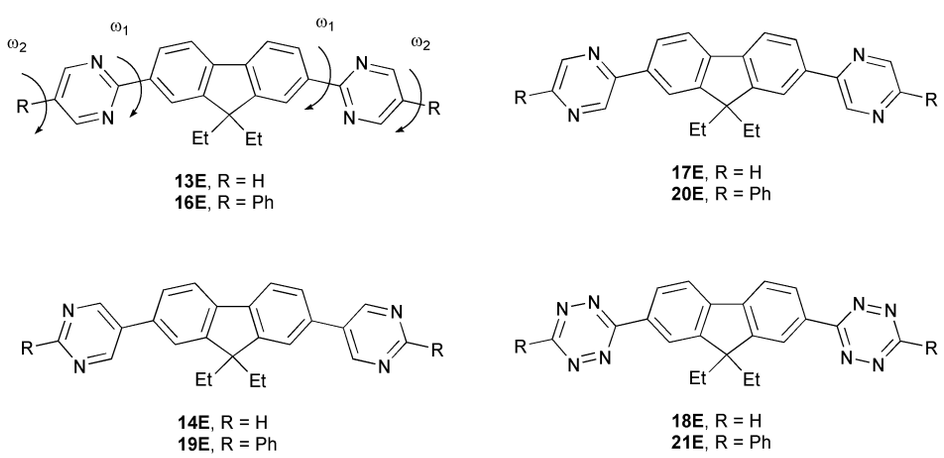

Chart 2 Structures of compounds **13E**, **14E**, **16E**–**21E** studied by *ab inito* calculations.

Thus, the calculated energy of the HOMO orbital (Table 2) for **14** is 0.41–0.45 eV lower than that of **13**, so its E_{pa} value is estimated to be around +(1.91–1.96 V) which is out of the range of the electrochemical transparency of DCM.

The estimated HOMO–LUMO gaps for all compounds **13**–**16** from their optical spectra are higher than 3 eV, therefore, reduction is predicted to occur at potentials around −2 V, which is out of the window of electrochemical transparency of DCM, so it is not possible to experimentally determine the electrochemical band gap for these compounds (although E_{red} values for some oligo/poly-fluorenes were measured in THF or acetonitrile [33]).

Quantum chemical calculations

For modelling compounds **13**, **14** and **16**, geometries and electronic structures were calculated for compounds **13E**,**14E**, and **16E** which have ethyl substituents at C(9) instead of hexyl. In addition, the same calculations were performed for derivatives **17E**–**21E**, to study the influence of the position and the number of nitrogen atoms in the heterocycle attached to the fluorene moiety (Chart 2).

Ab initio calculations of the geometries and electronic structures were performed at the HF and DFT levels of theory at HF/6-31G(d,p), B3LYP/6-31G(d,p) and B3PW91/6-31G(d,p). Both DFT methods (B3LYP and PW91) gave similar results for the optimised geometries and electronic structures of the compounds (Table 2). Electronic structures were also calculated at the HF/6-31G(d,p)//B3LYP/6-31G(d,p) level (Fig. 8).

Both HF and DFT calculations indicate that the 2-pyrimidyl ring in the optimised geometries of **13E** and **16E** is in the plane of the fluorene moiety ($\omega_1 \approx 0°$). These results correspond well with experimental X-ray structural data for **16**, which showed only small deviations of the pyrimidine rings from the plane of the fluorene moiety (5.1° and 5.6°, Fig. 3). These small experimental distortions could probably be a result of crystal packing (in any case, the expected energy loss for such distortions is quite low). Their isomers **14E** and **19E**, however, have a

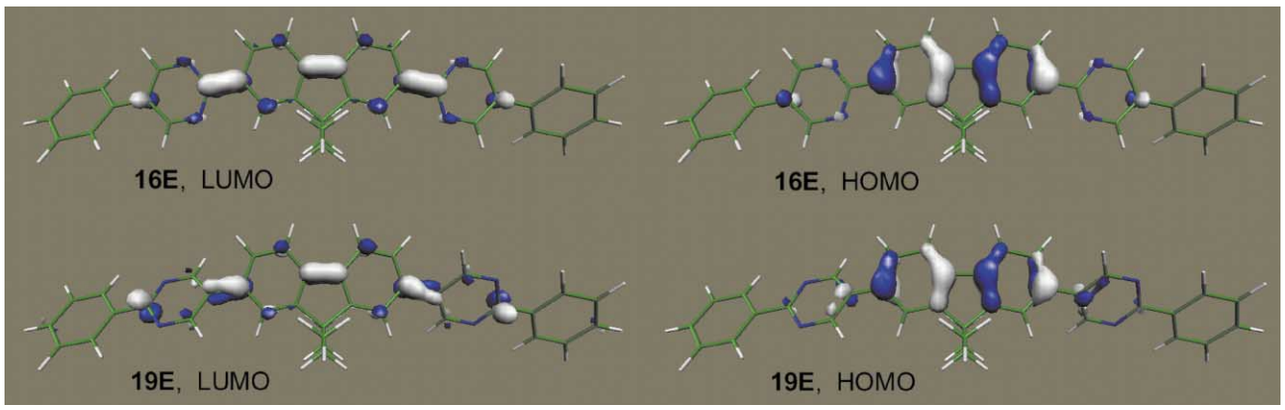

Fig. 8 Frontier orbitals of compounds **16E** and **19E** calculated by HF/6-31G(d,p)//B3LYP/6-31G(d,p) *ab initio* methods.

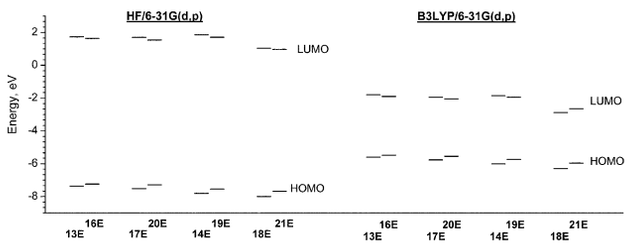

Fig. 9 Energy level diagram of compounds **13E**,**14E**, and **16E**–**21E**.

twisted structure with the dihedral angle between the 1,3-pyrimidin-5-yl ring and fluorene moiety ω_1 *ca.* 45° (HF) or 37° (DFT) (Table 2).[34] Again, these values are in the normal range of distortions in biphenyls (see above Crystal structures section). On the other hand, the ω_2 dihedral angle in **16E** between the phenyl ring and the planar pyrimidine-fluorene moiety is also pronounced (≈ 45° and ≈ 37° by HF and DFT, respectively) whereas in **19E** the phenyl-pyrimidine moiety is completely planar ($\omega_2 = 0°$). Thus, as seen in the crystal structures discussed above, the nitrogen atoms in the pyrimidine fragment decrease the steric repulsion which exists between adjacent benzene rings in biphenyl derivatives resulting in planarisation and hence facilitating conjugation between the aromatic rings in oligo(arylenes). This effect is clearly illustrated by the fluorene-tetrazine derivative **21E**, which represents a fully planar system ($\omega_1 = \omega_2 = 0°$). Pyrazine derivatives **17E** and **20E**, which have only one nitrogen atom adjacent to the fluorene or phenyl ring, have dihedral angles ω_1 and ω_2 of 28–29° and 19–21° by HF and DFT, respectively (Table 2) which are intermediate between those observed for phenyl and 2-phenylpyrimidine moieties.

A HOMO–LUMO energy diagram (Fig. 9) shows that, at both HF and DFT levels of theory, HOMO energies are monotonously decreased in the sequence **13E** > **17E** > **14E** > **18E** (and for phenyl-substituted derivatives **16E** > **19E** > **20E** > **21E**). In contrast, changes in LUMO energies are less pronounced for pyrimidine and pyrazine derivatives (**13E**, **14E**, **16E**, **17E**, **19E**, **20E**) but decreased for tetrazine derivatives **18E** and **21E**. At HF level, an addition of terminal phenyl substituents in all these series increased the HOMO and decreased the LUMO orbital energies, thus resulting in a contraction of the HOMO–LUMO gap (Table 2, Fig. 9). A similar tendency was observed in DFT calculations, however, for tetrazine derivatives an addition of terminal phenyl substituent (**18e**⟶**21E**) resulted in increasing LUMO energy (nevertheless the HOMO–LUMO gap decreased). Although the exact physical meaning of DFT orbital energies is a controversial subject[35] and B3LYP/6-31G(d,p) gave too high energies for the HOMO orbitals, it gives quite reliable HOMO–LUMO energy gaps, consistent with the spectroscopic data.

Analysis of the frontier orbital reveals that for all these compounds the HOMOs, which are located at the fluorene moiety, populate on the same carbon atoms of the benzene rings (Fig. 8, Figs. S-1–S-8 in ESI †), whereas the LUMOs are localised at C–C bonds between the 6-membered aromatic rings. Therefore, HOMO–LUMO excitation should increase the quinoidal character of the system, especially the central fluorene moiety. As a result of planarity between the pyrimidine and fluorene rings in **13E** and **16E** the population of the LUMO on the C–C bonds between these rings is more pronounced than that for **14E** and **19E**, where the dihedral angle ω_1 is quite large (Table 2).

Conclusions

A series of new pyrimidine-containing oligo(arylenes) has been synthesised by Suzuki cross-coupling methodology and shown to possess interesting X-ray structural, photophysical and electronic properties. Theoretical calculations for pyrimidine, pyrazine and tetrazine derivatives establish that the nitrogen atoms decrease steric repulsion which exists in biphenyl derivatives resulting in planarisation of the system. Compound **16** has been used as the emissive layer in an OLED: at a high turn-on voltage blue-green light (λ_{max} 500 nm) is emitted which most likely emanates primarily from excimer states. Our synthetic methodology is versatile and further chemical modifications within this class of oligomers are underway to provide new materials with tunable optoelectronic and photophysical properties.

Experimental

General

The details are the same as those we reported recently.[5c]

Synthesis

Syntheses of compounds **4**, **9** and **10** are given in the ESI †.

5-Bromo-2-phenylpyrimidine (6) and 2,5-diphenylpyrimidine (7)

2,5-Dibromopyrimidine **4** (190 mg, 0.8 mmol) and benzeneboronic acid **5** (293 mg, 2.4 mmol) were dissolved in freshly distilled THF (15 cm^3) and then $Pd(PPh_3)_4$ (40 mg) was added and the mixture was stirred at 20 °C for 2 min. Sodium carbonate solution (1 M, 2 cm^3) was then added and the mixture was stirred at 70 °C for 50 h under Ar. After cooling to room temperature, THF was evaporated and the resulting aqueous suspension of compounds **6** and **7** was suction filtered to obtain a white solid which was washed with water and then with hexane. This crude product was chromatographed on silica (DCM–hexane, 1 : 1 v/v). Removing the solvent and recrystallisation of the residue from toluene yielded pure compound **7** (60 mg, 32%) as colourless crystals, mp 185.0–185.5 °C (lit.,[16b] 180–181 °C). *m*/*z* (EI) 232 (M^+, 100%). δ_H ($CDCl_3$) 7.45 (t, 2H,

Table 3 Crystal data for compounds **6**, **7**, and **15**

Compound	**6**	**7**	**15**
Formula	$C_{10}H_7BrN_2$	$C_{16}H_{12}N_2$	$C_{33}H_{36}Br_2N_2$
Formula weight	235.09	232.28	648.48
T/ K	120	103	100
Symmetry	Monoclinic	Monoclinic	Triclinic
Space group	$P2_1/c$ (# 14)	$I2/a$ (# 15)	$P\bar{1}$ (# 2)
a/ Å	6.271(1)	7.444(2)	10.244(3)
b/ Å	21.359(3)	5.731(2)	10.979(3)
c/ Å	6.932(1)	26.932(8)	13.520(3)
α (°)	90	90	93.37(1)
β (°)	108.27(1)	92.82(1)	93.99(1)
γ (°)	90	90	95.14(1)
V/ Å^3	881.7(2)	1147.6(6)	1507.6(7)
Z	4	4	2
μ/ mm^{-1}	4.61	0.08	2.72
Reflections collected	10386	4867	16402
Unique reflections	2358	1528	6944
R_{int}	0.052 (0.102[a])	0.029	0.119 (0.158[a])
Reflections $F^2>2\sigma(F^2)$	2004	1263	5144
$R[F^2>2\sigma(F^2)]$	0.029	0.042	0.094
w$R(F^2)$, all data	0.079	0.123	0.278

[a] Before absorption correction.

J_o = 8 Hz), 7.52 (m, 4H), 7.64 (d, 2H, J_o = 8 Hz), 8.50 (dd, 2H, J_m = 2 Hz, J_o = 7.5 Hz), 9.03 (s, 2H). δ_C ($CDCl_3$) 127.07, 128.11, 128.76, 129.55, 130.70, 155.41, 155.91.

The combined mother toluene liquor and DCM–hexane eluate (apart from the DCM–hexane solution of product **7**) was evaporated and the residue was chromatographed on silica (eluent DCM–petroleum ether, 1 : 1 v/v) to yield **6** as a white crystalline solid (from ethanol) (80 mg, 43% yield) mp 104.0–104.5 °C (lit.,[16a] mp 104–105 °C). *m*/*z* (EI) 234 (M^+[^{79}Br], 100%,),) 236 (M^+[^{79}Br], 93%). δ_H ($CDCl_3$) 7.50 (m, 3H), 8.40 (m, 2H), 8.84, (s, 2H). δ_C ($CDCl_3$) 118.29, 128.13, 128.69, 131.12, 136.45, 157.82, 162.84.

Using benzeneboronic acid (2.0 eq.), $Pd_2(dba)_3$ P(Bu^t)$_3$ as catalyst in THF at 20 °C, and workup as described above, afforded compound **7** in 62% yield.

2,7-Bis(2-pyrimidyl)-9,9-dihexylfluorene 13

To a solution of 2-bromopyrimidine **11** (0.28 g, 1.78 mmol) in freshly distilled THF (30 cm^3) was added $Pd(PPh_3)_4$ (69 mg) and the mixture was stirred at 20 °C for 30 min. Compound **10** (0.25 g, 0.60 mmol) and Na_2CO_3 (1 M, aqueous, degassed, 2.5 cm^3) were added sequentially. The mixture was stirred at 70 °C for 30 h to give a yellow solution. The solvent was evaporated and water (100 cm^3) added to the residue which was extracted into DCM (3 × 50 cm^3). The organic layer was dried ($MgSO_4$) then concentrated under reduced pressure and purified by chromatography on a silica column (eluent DCM–ethyl acetate, 9 : 1 v/v) to yield compound **13** as a yellow solid (100 mg, 34% yield) mp 155–157 °C. *m*/*z* (EI) 490 (M^+, 100%). HRMS (EI) (M^+) 490.30946 (calcd. for $C_{33}H_{38}N_4$: 490.30965). δ_H ($CDCl_3$) 0.66 (m, 10H), 0.93 (m, 12H), 2.07 (m, 4H, *J* = 8.0 Hz), 7.16 (t, 2H, *J* = 4.8 Hz), 7.81 (d, 2H, *J* = 8.0 Hz), 8.39 (s, 2H), 8.45 (d, 2H, *J* = 8.0 Hz), 8.78 (d, 4H, *J* = 4.9 Hz). δ_C ($CDCl_3$) 13.95, 22.56, 23.71, 29.69, 31.48, 40.36, 55.55, 118.84, 120.35, 122.44, 127.40, 136.75, 143.28, 152.07, 157.23, 164.97.

2,7-Bis(5-pyrimidyl)-9,9-dihexylfluorene 14

By analogy with the synthesis of **13**, 5-bromopyrimidine **12** (0.28 g, 1.78 mmol), THF (30 cm^3), $Pd(PPh_3)_4$ (69 mg) compound **10** (0.25 g, 0.60 mmol) and Na_2CO_3 (1 M, degassed, 2.5 cm^3) gave compound **14** as a yellow solid (93 mg, 32% yield), mp 157–158 °C. *m*/*z* (EI) 490 (M^+, 100%). HRMS (EI) (M^+) 490.31014 (calcd. for $C_{33}H_{38}N_4$: 490.30965). δ_H ($CDCl_3$) 0.65 (m, 10H), 1.00 (m, 12H), 2.01 (m, 4H, *J* = 8.0 Hz), 7.50 (s, 2H), 7.53 (d, 2H, *J* = 8.0 Hz), 7.81 (d, 2H, *J* = 7.6 Hz), 8.97 (s, 4H), 9.17 (s, 2H). δ_C ($CDCl_3$) 14.20, 22.75, 24.05, 29.79, 31.65, 40.50, 55.93, 121.46, 126.40, 128.82, 132.52, 133.74, 141.32, 152.65, 155.14, 157.49.

2,7-Bis(5-bromo-2-pyrimidyl)-9,9-dihexylfluorene 15

By analogy with the synthesis of **13**, 2,5-dibromopyrimidine **4** (0.42 g, 1.78 mmol), THF (30 cm^3), $Pd(PPh_3)_4$ (68 mg), compound **10** (0.25 g, 0.60 mmol) and Na_2CO_3 (1 M, degassed, 2.5 cm^3) and chromatography (eluent DCM–petroleum ether, 9 : 1 v/v) gave a white solid, which was recrystallised from hexane to yield compound **15** as white needles (87 mg, 23% yield), mp 179.3–179.8 °C. *m*/*z* (EI) 648 (M^+, 100%). HRMS (EI) (M^+) 646.13040 (calcd. for $C_{33}H_{36}Br_2N_4$: 646.13067). δ_H ($CDCl_3$) 0.68 (m, 10H), 1.01 (m, 12H), 2.12 (m, 4H, *J* = 8.5 Hz), 7.85 (d, 2H, *J* = 8.5 Hz), 8.41 (s, 2H), 8.47 (d, 2H, *J* = 8.2 Hz), 8.86 (s, 4H). δ_C ($CDCl_3$) 13.96, 22.55, 23.81, 29.66, 31.48, 40.28, 55.55, 117.95, 120.48, 122.51, 127.48, 135.86, 143.45, 152.18, 157.78, 163.08.

2,7-Bis(5-phenyl-2-pyrimidyl)-9,9-dihexylfluorene 16

To a solution of compound **15** (100 mg, 0.154 mmol) in freshly distilled THF (30 cm^3) was added $Pd(PPh_3)_4$ (53.5 mg) and the mixture was stirred at 20 °C for 30 min. Benzeneboronic acid **5** (60 mg, 0.46 mmol) and Na_2CO_3 (1 M, aqueous degassed, 2.0 cm^3) were added sequentially. Reaction and workup as described for **13** followed by column chromatography on silica gel (eluent DCM–petroleum ether, 4 : 1 v/v) gave compound **16** as a pale yellow solid (35 mg, 35% yield), mp 185.5–186.5 °C. *m*/*z* (EI) 642 (M^+, 100%). HRMS (EI) (M^+) 642.37197 (calcd. for $C_{45}H_{46}N_4$: 642.37225). δ_H ($CDCl_3$) 0.71 (m, 10H), 1.07 (m, 12H), 2.19 (m, 4H, *J* = 8.0 Hz), 7.47 (m, 2H), 7.54 (t, 4H, *J* = 7.0 Hz), 7.65 (d, 4H, *J* = 11.5 Hz), 7.91 (d, 2H, *J* = 8.0 Hz), 8.53 (s, 2H), 8.58 (d, 2H, *J* = 8.0 Hz), 9.07 (s, 4H). δ_C ($CDCl_3$) 13.96, 22.57, 23.85, 29.72, 31.53, 40.41, 55.58, 120.41, 122.38, 126.70. 127.40 128.70, 129.40, 131.38, 134.59, 136.54, 143.28, 152.12, 155.17, 163.69.

X-Ray crystallography

X-Ray diffraction experiments (see Table 3 ‡) were carried out on a SMART 3-circle diffractometer with a 1K CCD area detector, with graphite-monochromated Mo-K_α radiation (λ = 0.71073 Å) and a Cryostream open-flow N_2 cryostat (Oxford Cryosystems). The full sphere of reciprocal space was covered by five sets of 0.3° ω scans, each set with different ϕ and/or 2θ angles. The

data of **6** and **15** were corrected for absorption by numerical integration based on real crystal shape. The diffraction data of **15** carries internal signs of twinning, which we were unable to rationalize. This (or an imperfect absorption correction) is probably responsible for the relatively high final R and four residual peaks of electron density (2.84 to 4.34 $eÅ^{-3}$) at distances of 0.96 to 0.99 Å from both bromine atoms. The structures were solved by direct methods and refined by full-matrix least squares against F^2 of all data, using SHELXTL software.

Photoluminescence measurements

Photoluminescence spectra were recorded using a Jobin-Yvon Horiba Fluorolog 3–22 Tau-3 spectrofluorimeter with a 0.5–2 nm bandpass using a Xenon lamp. Spectra were recorded using conventional 90° geometry with an excitation at 355 nm. The film PLQY were measured using a Jobin-Yvon Fluoromax spectrofluorimeter equipped with an integrating sphere.[36] The standards for PLQY were quinine sulfate (Φ = 0.577 in 0.1 M H_2SO_4) and β-carbolene (Φ = 0.60 in 0.5 M H_2SO_4), and excitation was at 350 nm in both cases.

Fabrication of light-emitting devices

A hole-conducting poly(ethylenedioxythiophene) (PEDOT) layer (30 nm thick) was spun onto an etched ITO glass substrate (20 Ω/□), and then baked overnight in a vacuum oven at 50 °C to remove residual water. A dilute solution of compound **16** in toluene (*ca.* 0.5 mg cm^{-3}) was then drop-cast onto the PEDOT to form an active layer (*ca.* 300 nm thick, as confirmed by AlphaStep measurements). On top of this layer, a cathode of 50 nm thick calcium capped with 50 nm thick aluminium was deposited by evaporation under high vacuum.

Electrochemical measurements

Cyclic voltammetry experiments were performed on a BAS CV50W electrochemical analyzer with *iR* compensation. Platinum wire, platinum disk (∅ 1.6 mm) and Ag/Ag^+ were used as counter, working, and reference electrodes, respectively. CV experiments were performed in dry dichloromethane with 0.2 M $Bu_4N^+PF_6^-$ as supporting electrolyte; concentrations of compounds were *ca.* 10^{-3} M^{-1}. The scan rate was varied from 50 to 500 mV s^{-1}. The potentials were referenced to Fc/Fc^+ couple as the internal reference, which showed a potential of +0.17 V *vs.* Ag/Ag^+ in our conditions.

Computational procedure

The *ab initio* computations were carried out with the Gaussian 98[37] package of programs at both Hartree–Fock and density-functional theory levels using Pople's 6–31G split valence basis set supplemented by *d*-polarisation functions on heavy atoms and *p*-polarisation functions on hydrogens. DFT calculations were carried out using Becke's three-parameter hybrid exchange functional[38] with either Lee–Yang–Parr correlation functional[39] (B3LYP) or Perdew–Wang 1991 gradient-corrected correlation functional[40] (B3PW91). Geometries were optimised with HF/6-31G(d,p), B3LYP/6-31G(d,p) and B3PW91/6-31G(d,p) and electronic structures were calculated at the same levels. Contours of HOMO and LUMO orbitals were also calculated at HF/6-31G(d,p)//B3LYP/6-31G(d,p) level and visualisation of frontier orbital populations was performed using Molekel v.4.2 program.[41] No constraints of bonds/angles/dihedral angles were applied in the calculations and all the atoms were free to optimise.

Acknowledgements

We thank EPSRC for funding; The Royal Society (RS-NASU Exchange Program) and The Royal Society of Chemistry (Journals Grant for International Authors) for funding visits by I. F. P. to Durham; B. P. L. thanks Sony Europe plc for providing a CASE studentship; A. P. M. thanks the Leverhulme Foundation for a fellowship. M. R. B. and A. P. M. thank Durham County Council under the Science and Technology for Business and Enterprise Programme SP/082 for funding the purchase of equipment used in this work.

References

1 Review: Y. Shirota, *J. Mater. Chem.*, 2000, **10**, 1.
2 Reviews: (*a*) A. Kraft, A. C. Grimsdale and A. B. Holmes, *Angew. Chem., Int. Ed.*, 1998, **37**, 402; (*b*) U. Mitschke and P. Bäuerle, *J. Mater. Chem.*, 2000, **10**, 1471.
3 Review: D. Fichou, *J. Mater. Chem.*, 2000, **10**, 571.
4 Review: M. Thelakkat and H.-W. Schmidt, *Polym. Adv. Technol.*, 1998, **9**, 429.
5 (*a*) Z. Peng, Z. Bao and M. E. Galvin, *Chem. Mater.*, 1998, **10**, 2086; (*b*) C. Wang, M. Kilitziraki, L.-O. Pålsson, M. R. Bryce, A. P. Monkman and I. D. W. Samuel, *Adv. Funct. Mater.*, 2001, **11**, 47; (*c*) C. Wang, G.-Y. Jung, A. S. Batsanov, M. R. Bryce and M. C. Petty, *J. Mater. Chem.*, 2002, **12**, 173.
6 (*a*) J. K. Kim, J. W. Yu, J. M. Hong, H. N. Cho, D. Y. Kim and C. Y. Kim, *J. Mater. Chem.*, 1999, **9**, 2171; (*b*) J. A. Irvin, C. J. DuBois and J. R. Reynolds, *Chem. Commun.*, 1999, 2121; (*c*) C. Wang, M. Kilitziraki, J. A. H. MacBride, M. R. Bryce, L. Horsburgh, A. Sheridan, A. P. Monkman and I. D. W. Samuel, *Adv. Mater. (Weinheim, Ger.)*, 2000, **12**, 217; (*d*) A. P. Monkman, L.-O. Pålsson, R. W. T. Higgins, C. Wang, M. R. Bryce and J. A. K. Howard, *J. Am. Chem. Soc.*, 2002, **124**, 6049.
7 (*a*) X. Zhang, A. S. Shetty and S. A. Jenekhe, *Acta Polym.*, 1998, **49**, 52; (*b*) X. Zhang and S. A. Jenekhe, *Macromolecules*, 2000, **33**, 2069.
8 K. R. J. Thomas, J. T. Lin, Y-T. Tao and C. H. Chuen, *J. Mater. Chem.*, 2002, **12**, 3516.
9 (*a*) T. Kanbara, T. Kushida, N. Saito, I. Kuwayiama, K. Kubota and T. Yamamoto, *Chem. Lett.*, 1992, 583; (*b*) C. C. Wu, Y. T. Lin, H. H. Chiang, T. Y. Cho, C. W. Chen, K. T. Wong, Y. L. Liao, G. H. Lee and S. M. Peng, *Appl. Phys. Lett.*, 2002, **81**, 577.
10 R. Gompper, H. Mair and K. Polborn, *Synthesis*, 1997, 696.
11 (*a*) M. T. Bernius, M. Inbasekaran, J. O'Brien and W. Wu, *Adv. Mater. (Weinheim, Ger.)*, 2000, **12**, 1737; (*b*) S. Destri, M. Pasini, C. Botta, W. Porzio, F. Bertini and L. Marchio, *J. Mater. Chem.*, 2002, **12**, 924; (*c*) Review: U. Scherf and E. J. W. List, *Adv. Mater. (Weinheim, Ger.)*, 2002, **14**, 477; (*d*) D.-H Hwang, J.-D Lee, J.-M. Kang, S. Lee, C.-H. Lee and S.-H. Jin, *J. Mater. Chem.*, 2003, **13**, 1540.
12 (*a*) S. W. Chang, J.-M. Hong, J. W. Hong and H. N. Choi, *Polym. Bull.*, 2001, **47**, 231; (*b*) S. Beaupré, M. Ranger and M. Leclerc, *Macromol. Rapid Commun.*, 2000, **21**, 1013; (*c*) H. N. Cho, J. K. Kim, D. Y. Kim, C. Y. Kim, N. W. Song and D. Kim, *Macromolecules*, 1999, **32**, 1476; (*d*) M. Ranger, D. Rondeau and M. Leclerc, *Macromolecules*, 1997, **30**, 7686.
13 For a review of cross-coupling methodology in oligomer/polymer synthesis see: (*a*) A. D. Schluter, *J. Polym. Sci., Part A: Polym. Chem.*, 2001, **39**, 1533; (*b*) J. Hassan, M. Sévignon, C. Gozzi, E. Schulz and M. Lemaire, *Chem. Rev.*, 2002, **102**, 1359.
14 (*a*) D. J. Brown and J. M. Lyall, *Aust. J. Chem.*, 1964, **17**, 794; (*b*) B. W. Arantz and D. J. Brown, *J. Chem. Soc., C*, 1971, 1889; (*c*) H. Schlosser and R. Wingen, U. S. Patent, 5,371,224, 1994.
15 (*a*) G. Cooke, H. A. de Cremiers, V. M. Rotello, B. Tarbit and P. E. Vanderstraeten, *Tetrahedron*, 2001, **57**, 2787; (*b*) J. M. Schoemaker and T. J. Delia, *J. Org. Chem.*, 2001, **66**, 7125; (*c*) K.-T. Wong, T. S. Hung, Y. Lin, C.-C. Wu, G.-H. Lee, S.-M. Peng, C. H. Chou and Y. O. Su, *Org. Lett.*, 2002, **4**, 513; (*d*) P. M. Murphy, V. A. Phillips, S. A. Jennings, N. C. Garbett, J. B. Chaires, T. C. Jenkins and R. T. Wheelhouse, *Chem. Commun.*, 2003, 1160.
16 (*a*) Compound **6**: J. Nasielski, A. Kirsh-Demesmaeker and R. Nasielski-Hinkens, *Tetrahedron*, 1972, **28**, 3767; (*b*) Compound **7**: R. M. Wagner and C. Jutz, *Chem. Ber.*, 1971, **104**, 2975.
17 A. F. Littke, C. Dai and G. C. Fu, *J. Am. Chem. Soc.*, 2000, **122**, 4020.
18 For alternative procedures for alkylation of 2,7-dibromofluorene to yield **9** see: (*a*) W.-Y. Wong, K.-H. Choi, G.-L. Lu, J.-X. Shi, P.-Y. Lai and S.-M. Chan, *Organometallics*, 2001, **20**, 5446; (*b*) W.-Y. Wong, G.-L. Lu, K.-H. Choi and J.-X. Shi, *Macromolecules*, 2002, **35**, 3506; (*c*) S. H. Lee and T. Tsutsui, *Thin Solid Films*, 2000, **363**, 76; (*d*) W.-L. Yu, J. Pei, Y. Cao, W. Huang and A. J. Heeger, *Chem. Commun.*, 1999, 1837; (*e*) M. Ranger and M. Leclerc, *Chem. Commun.*, 1997, 1597.
19 For alternative procedures of obtaining compound **10** from **9** see: (*a*) Ref. 18*d*.; (*b*) B. Liu, W.-L. Yu, Y.-H. Lai and W. Huang,

Macromolecules, 2000, **33**, 8945; (*c*) X. Zhan, Y. Liu, D. Zhu, W. Huang and Q. Gong, *Chem. Mater.*, 2001, **13**, 1540.
20 (*a*) H. Cailleau, J. L. Baudour and C. M. E. Zeyen, *Acta Crystallogr., Sect. B: Struct. Crystallogr. Cryst. Chem.*, 1979, **35**, 426; (*b*) G. Häfelingen and C. Regelmann, *J. Comput. Chem.*, 1985, **6**, 368; (*c*) G. Häfelingen and C. Regelmann, *J. Comput. Chem.*, 1987, **8**, 1057; (*d*) Y. Takei, T. Yamaguchi, Y. Osamura, K. Fuke and K. Kaya, *J. Phys. Chem.*, 1988, **92**, 577.
21 (*a*) O. Bastiansen, *Acta Chem. Scand.*, 1950, **4**, 926; (*b*) O. Bastiansen, *Acta Chem. Scand.*, 1950, **4**, 926; (*c*) O. Bastiansen and M. Traetenberg, *Tetrahedron*, 1962, **17**, 147.
22 E. D. Schmid and B. Brosa, *J. Chem. Phys.*, 1972, **56**, 6267.
23 (*a*) R. M. Barrett and D. Steele, *J. Mol. Struct.*, 1972, **11**, 105; (*b*) V. J. Eaton and D. Steele, *J. Chem. Soc., Faraday Trans. 2*, 1973, **69**, 1601.
24 (*a*) G.-P. Charbonneau and Y. Delugeard, *Acta Crystallogr., Sect. B: Struct. Crystallogr. Cryst. Chem.*, 1976, **32**, 1420; (*b*) G.-P. Charbonneau and Y. Delugeard, *Acta Crystallogr., Sect. B: Struct. Crystallogr. Cryst. Chem.*, 1977, **33**, 1586.
25 (*a*) I. Rapthel, H. Hartung, R. Richter and M. Jaskolski, *J. Prakt. Chem./Chem. Ztg.*, 1983, **325**, 489; (*b*) G. Winter, H. Hartung and M. Jaskolski, *Mol. Cryst. Liq. Cryst.*, 1987, **149**, 17; (*c*) G. Winter, H. Hartung, W. Brandt and M. Jaskolski, *Mol. Cryst. Liq. Cryst.*, 1987, **150**, 289; (*d*) P. Mandal, B. Majumdar, S. Paul, H. Schenk and K. Goubitz, *Mol. Cryst. Liq. Cryst.*, 1989, **168**, 135; (*e*) P. Mandal, S. Paul, S. H. Stam and H. Schenk, *Mol. Cryst. Liq. Cryst., Sect. B*, 1990, **180B**, 369; (*f*) A. M. Babu, S. B. Bellad, M. A. Sridhar, A. Indira, M. S. Madhava and J. S. Prasad, *Z. Kristallogr.*, 1992, **202**, 25.
26 R. Anémain, J.-C. Mulatier, C. Andraud, O. Stéphan and J-C. Vial, *Chem. Commun.*, 2002, 1608.
27 Q. Hou, Y. Xu, W. Yang, M. Yuan, J. Peng and Y. Cao, *J. Mater. Chem.*, 2002, **12**, 2887.
28 H. S. Woo, J. G. Lee, H. K. Min, E. J. Oh, S. J. Park, K. W. Lee, J. H. Lee, S. H. Cho, T. W. Kim and C. H. Park, *Synth. Met.*, 1995, **71**, 2173.
29 J. H. Hsu, W. S. Fann, H. F. Meng, E. S. Chen, E. C. Chang, S. A. Chen and K. W. To, *Chem. Phys.*, 2001, **269**, 367.
30 V. Adamovich, J. Brocks, A. Tamayo, A. M. Alexander, P. I. Djurovich, B. W. S'Andrade, C. Adachi, S. R. Forrest and M. E. Thompson, *New J. Chem.*, 2002, **26**, 1171.
31 E. J. W. List, R. Guentner, P. Scanducci de Freitas and U. Scherf, *Adv. Mater. (Weinheim, Ger.)*, 2002, **14**, 374.
32 L.-O. Pålsson, C. Wang, D. L. Russel, A. P. Monkman, M. R. Bryce, G. Rumbles and I. D. W. Samuel, *Chem. Phys.*, 2002, **279**, 229 and references therein.
33 (*a*) K.-T. Wong, Y.-Y. Chien, R.-T. Chen, C.-F. Wang, Y.-T. Lin, H.-H. Chiang, P.-Y. Hsieh, C.-C. Wu, C. H. Chou, Y. O. Su, G.-H. Lee and S.-M. Peng, *J. Am. Chem. Soc.*, 2002, **124**, 11576; (*b*) J. Pei, W.-L. Yu, W. Huang and A. J. Heeger, *Chem. Commun.*, 2000, 1631; (*c*) J. K. Kim, J. W. Yu, J. M. Hong, H. N. Cho, D. Y. Kim and C. Y. Kim, *J. Mater. Chem.*, 1999, 2171; (*d*) I. Prieto, J. Teetsov, M. A. Fox, D. A. Vanden Bout and A. J. Bard, *J. Phys. Chem. A*, 2001, **105**, 520.
34 HF/6-31G(d) calculated dihedral angles between the phenyl substituents and the fluorene moiety in 2,7-diphenyl-9,9-dioctyl-fluorene were found to be 45.5°: M. Belletete, J.-F. Morin, S. Beaupre, M. Leclerc and G. Durocher, *Synth. Met.*, 2002, **126**, 43.
35 U. Salzner, *J. Phys. Chem. B*, 2002, **106**, 9214 and references cited therein.
36 L.-O. Pålsson and A. P. Monkman, *Adv. Mater. (Weinheim, Ger.)*, 2002, **14**, 757.
37 M. J. Frisch, G. W. Trucks, H. B. Schlegel, G. E. Scuseria, M. A. Robb, J. R. Cheeseman, V. G. Zakrzewski, J. A. Montgomery, Jr., R. E. Stratmann, J. C. Burant, S. Dapprich, J. M. Millam, A. D. Daniels, K. N. Kudin, M. C. Strain, O. Farkas, J. Tomasi, V. Barone, M. Cossi, R. Cammi, B. Mennucci, C. Pomelli, C. Adamo, S. Clifford, J. Ochterski, G. A. Petersson, P. Y. Ayala, Q. Cui, K. Morokuma, D. K. Malick, A. D. Rabuck, K. Raghavachari, J. B. Foresman, J. Cioslowski, J. V. Ortiz, B. B. Stefanov, G. Liu, A. Liashenko, P. Piskorz, I. Komaromi, R. Gomperts, R. L. Martin, D. J. Fox, T. Keith, M. A. Al-Laham, C. Y. Peng, A. Nanayakkara, C. Gonzalez, M. Challacombe, P. M. W. Gill, B. G. Johnson, W. Chen, M. W. Wong, J. L. Andres, M. Head-Gordon, E. S. Replogle and J. A. Pople, GAUSSIAN 98 (Revision A.9), Gaussian, Inc., Pittsburgh, PA, 1998.
38 A. D. Becke, *Phys. Rev. A*, 1988, **38**, 3098; A. D. Becke, *J. Chem. Phys.*, 1993, **98**, 5648.
39 C. Lee, W. Yang and R. G. Parr, *Phys. Rev. B*, 1988, **37**, 785.
40 J. P. Perdew and Y. Wang, *Phys. Rev. B*, 1992, **45**, 13244; J. P. Perdew, in *Electronic Structure of Solids '91*, ed. P. Ziesche and H. Eschrig, Akademie Verlag, Berlin, 1991, p. 11.
41 (*a*) P. Flükiger, H. P. Lüthi, S. Portmann and J. Weber, Molekel, Version 4.2, Swiss Center for Scientific Computing, Manno (Switzerland), 2000; http://www.cscs.ch/molekel/; (*b*) S. Portmann and H. P. Lüthi, *Chimia*, 2000, **54**, 766.